Close-range maneuver planning for uncontrolled rendezvous with multiple elliptical orbit targets based on genetic algorithm

Journal of Physics: Conference Series **2762** (2024) 012063 doi:10.1088/1742-6596/2762/1/012063

Close-range maneuver planning for uncontrolled rendezvous with multiple elliptical orbit targets based on genetic algorithm

Fuhong Xiao[1] Yanhong Sun[2] and Rixin Wang[1,*]

Deep Space Exploration Research Center, Harbin Institute of Technology, Harbin, China
China satellite network group CO. LTD.

Email: wangrx@hit.edu.cn

Abstract. On-orbit debris removal is an important and challenging problem in space engineering. A low-cost method for this problem is to use uncontrolled rendezvous with a sub-spacecraft released by a service spacecraft. The sub-spacecraft do not carry any control system and are designed to rendezvous with the target debris to remove it. This paper presents a comprehensive study on the mission planning. First, we analyze and dynamically model the uncontrolled rendezvous process for elliptical orbit targets, and study various aspects such as maneuver, sub-spacecraft release parameter solution, and rendezvous accuracy estimation. Then, we use NSGA-II, a multi-objective optimization genetic algorithm, to establish the mission planning model, focusing on the design of decision variables, constraints and fitness functions. Finally, we apply our proposed method to two specific cases of Molniya orbit, and verify the effectiveness of the planning model. We also conduct a deep analysis of the planning results, and summarize the commonalities and differences of various effective strategies.

Keywords: Uncontrolled rendezvous；Mission planning；Multiple on-orbit targets

1. Introduction

With the development of space exploration, the number of on-orbit debris has increased significantly. According to ESA’s Space Environment Report 2022[5], the estimated number of debris objects in orbit greater than 10 cm is approximately 34,000, which not only waste precious orbital resources, but also pose a great threat to the safety of spacecraft in orbit. As a result, the methods of removing on-orbit debris have become worth analyzing. Facing such a large number of targets, how to use as few resources as possible to clean up these targets is a very valuable research problem.

One method worth considering for cleaning up targets is to use a single satellite, release sub-spacecraft to rendezvous with the targets, and thus achieve target removal, as Figure 1. The sub-spacecraft should be as simple as possible to achieve the goal of saving resources as much as possible. When cleaning up targets, there are three aspects that need attention. First, the success rate of the cleanup. For the method of uncontrolled rendezvous of sub-spacecraft, the success rate depends on the accuracy of uncontrolled rendezvous. Second and third, the fuel consumption and time consumption of the mission. Facing multiple targets, it is necessary to plan the order of cleanup, the position and timing of releasing sub-spacecraft, so that the cost of cleaning up targets is within an acceptable range.

This method is essentially a kind of on-orbit service (OOS). It encompasses dynamic processes related to release and rendezvous, as well as strategic planning. The academic community has

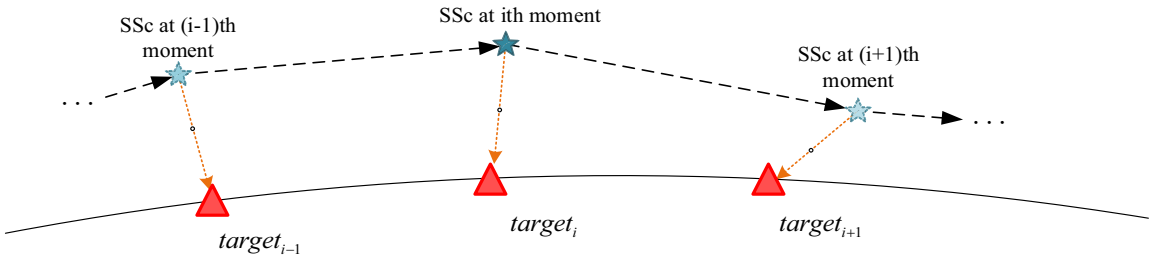

Figure 1. Schematic diagram of a uncontrol close-range rendezvous to multiple targets.

extensively researched this field. In the context of spacecraft release and separation dynamics, several studies have addressed critical aspects. Jeyakumar et al.[3] focused on satellite separation dynamics, Cui et al.[4] explored parameter sensitivity for separation, and Fan et al.[8] simulated safety during separation. Wang et al.[6] investigated satellite capture, akin to sub-spacecraft rendezvous, provides valuable insights. For rendezvous precision, Ma Yanhong[2] analyzed guidance system errors using the Clohessy-Wiltshire (CW) equation. Li[9] and Xie[10] studied spacecraft rendezvous precision in practical Chinese space engineering. In rendezvous planning, researchers often employ evolutionary algorithms (EAs) like genetic algorithms (GA)[12], or Neural-network-assisted optimization algorithm[7]. These methods typically focus on Service spacecraft (SSc) and target rendezvous. However, when releasing sub-spacecraft for debris cleanup, SSc need not approach the target spacecraft closely. The goal is to ensure sufficient proximity for accurate rendezvous with both the target spacecraft and sub-spacecraft.

The main structure of this paper is as follows. Chapter 2 analyzes the relative motion dynamics model of elliptical orbit targets and establishes mathematical models for maneuvering, accuracy estimation and release parameter solution. Chapter 3 introduces the specific details of establishing planning model using NSGA-II algorithm. Chapter 4 sets up examples and simulates mission planning in scenarios such as accompanying flight and glancing flight and analyzes specific strategies.

2. Uncontrolled rendezvous dynamical model

According to the scene this paper research, the precise of rendezvous is depend on the initial state of the SSc when release sub-spacecraft. We think there are two mainly source of initial error, the target observation error and sub-spacecraft releasing error. In order to analyze how the initial error influent the rendezvous error, relative dynamic is studied this chapter; then, the expression of rendezvous error are derived; finally, the relationship of the initial state of SSc and the rendezvous are researched.

2.1 Spacecraft state transition matrix

The Tschauner-Hempel (TH) equation can describe the proximity relative motion between the SSc and the target when the distance between them is much smaller than the radius of them and the target in an ellipse orbit. Utilize the Vehicle Velocity Local Horizontal (VVLH) coordinate system to describe the proximity relative motion, TH equation can express as follows.

$$\begin{bmatrix} \ddot{x} \\ \ddot{y} \\ \ddot{z} \end{bmatrix} = \begin{bmatrix} -k\omega^{3/2}x + 2\omega\dot{z} + \dot{\omega}z + \omega^2 x \\ -k\omega^{3/2}y \\ 2k\omega^{3/2}z - 2\omega\dot{x} - \dot{\omega}x + \omega^2 z \end{bmatrix} \tag{1}$$

Where the meaning of symbol as follow.

x, y, z is relative position of the tracking vehicle on the target vehicle, the $k, \omega, \dot{\omega}$ is model parameters, orbital angular velocity, orbital angular acceleration.

Solving this differential equation (1), the steps of which are described in reference[1] and expressed in the form of a transfer matrix, results in:

$$\begin{cases} \begin{bmatrix} \tilde{x}_t \\ \tilde{z}_t \\ \tilde{v}_{xt} \\ \tilde{v}_{zt} \end{bmatrix} = \mathbf{\Phi}_\theta \mathbf{\Phi}_{\theta 0}^{-1} \cdot \begin{bmatrix} \tilde{x}_0 \\ \tilde{z}_0 \\ \tilde{v}_{x0} \\ \tilde{v}_{z0} \end{bmatrix} \\ \begin{bmatrix} \tilde{y}_t \\ \tilde{v}_{yt} \end{bmatrix} = \frac{1}{\rho_{\theta-\theta_0}} \begin{bmatrix} c & s \\ -s & c \end{bmatrix}_{\theta-\theta_0} \begin{bmatrix} \tilde{y}_0 \\ \tilde{v}_{y0} \end{bmatrix} \end{cases} \tag{2}$$

where the expression of $\mathbf{\Phi}_\theta$ is:

$$\mathbf{\Phi}_\theta = \begin{bmatrix} 1 & -c\left(1+1/\rho\right) & s\left(1+1/\rho\right) & 3\rho^2 J \\ 0 & s & c & \left(2-3esJ\right) \\ 0 & 2s & 2c-e & 3\left(1-2esJ\right) \\ 0 & s' & c' & -3e\left(s'J+s/\rho^2\right) \end{bmatrix} \tag{3}$$

$\mathbf{\Phi}_{\theta 0}$ is the θ_0 replace θ in $\mathbf{\Phi}_\theta$.

The calculation method of each symbol in reference[1]. According to reference[1], this analytic solution holds for any elliptic and circle orbit.

Set the matrix A, matrix Q. The expression of A is given by:

$$A = \begin{bmatrix} \Phi_\theta & \mathbf{0} \\ \mathbf{0} & \Phi_{y\theta} \end{bmatrix}_{6\times 6} \tag{4}$$

$$\begin{bmatrix} \mathbf{r_t} \\ \mathbf{v_t} \end{bmatrix} = Q_t^{-1} A_t A_0^{-1} Q_0 \begin{bmatrix} \mathbf{r_0} \\ \mathbf{v_0} \end{bmatrix} \tag{5}$$

For ease of representation, let the matrix B

$$B_t B_0^{-1} = Q_t^{-1} A_t A_0^{-1} Q_0 \tag{6}$$

$$B = Q^{-1} A \tag{7}$$

Let

$$B_t B_0^{-1} = \begin{bmatrix} B_{11} & B_{12} \\ B_{21} & B_{22} \end{bmatrix} \tag{8}$$

Finally obtain:

$$\begin{bmatrix} \mathbf{r_t} \\ \mathbf{v_t} \end{bmatrix} = \begin{bmatrix} B_{11} & B_{12} \\ B_{21} & B_{22} \end{bmatrix} \begin{bmatrix} \mathbf{r_0} \\ \mathbf{v_0} \end{bmatrix} \tag{9}$$

Equation (9) is the orbital transfer matrix used in this paper.

2.2 Maneuver

Consider using single pulse maneuver to close to each target spacecraft. We analyze the motion of the SSc in the VVLH frame of the target spacecraft. From equation (9), we obtain the following expression:

$$B_{11}^{i+1} \mathbf{r}_i^{i+1} + B_{12}^{i+1} (\mathbf{v}_i^{i+1} + \Delta \mathbf{v}_i) = \mathbf{r}_{i+1}^{i+1} \tag{10}$$

Where $\mathbf{r}_i^{i+1}$ and $\mathbf{r}_{i+1}^{i+1}$ are the relative positions of SSc spacecraft in i th and (i+1) th moment with respect to the (i+1) th target spacecraft and $\mathbf{r}_{i+1}^{i+1}$ is the desired position for the maneuver, $\mathbf{v}_i^{i+1}$ is the relative velocity of SSc with respect to the (i+1) th target spacecraft before maneuver, B^{i+1} is the transition matrix from the i th to the (i+1) th moment, and is the i th pulse velocity that makes the SSc maneuver to $\mathbf{r}_{i+1}^{i+1}$. $\Delta \mathbf{v}_i$

So the $\Delta \mathbf{v}_i$ is given by:

$$\Delta \mathbf{v}_i = -\mathbf{v}_i^{i+1} - (B_{12}^{i+1})^{-1}(\mathbf{r}_{i+1}^{i+1} - B_{11}^{i+1}\mathbf{r}_i^{i+1}) \tag{11}$$

2.3 Release and rendezvous

From the momentum theorem, we have:

$$m\mathbf{v}_0^m + M\mathbf{v}_0^M = (m+M)\mathbf{v}' \tag{12}$$

Associating (9), (12) and simplifying, keeping only the equations we care about, we have:

$$B_{11}\mathbf{r}_0 + B_{12}\left(\frac{M}{M+m}\Delta\mathbf{v} + \mathbf{v}'\right) = \mathbf{r}_t \tag{13}$$

Assuming $|\Delta\mathbf{v}|$ is a constant value, there are only two degrees of freedom for $\Delta\mathbf{v}$, denoted as $\Delta\mathbf{v}(\alpha,\beta)$. α and β are the angles of elevation and azimuth which is unknowns to be solved.

Then the complete equation for solving α, β is :

$$\begin{cases} B_{11}\mathbf{r}_0 + B_{12}(\mathbf{v}' + \dfrac{M}{M+m}\Delta\mathbf{v}) = 0 \\ \Delta t = \Delta\varphi - e\Delta\sin(\varphi)\sqrt{\dfrac{a^3}{\mu}} \end{cases} \tag{14}$$

φ is the eccentric anomaly.

$\mathbf{r}_0$ is the position of the SSc under the VVLH system of the target spacecraft at the initial moment.

$\mathbf{v}'$ is the velocity of the SSc relative to the target spacecraft at the initial moment.

Δt is the time from the release of the sub-spacecraft to the whole process of rendezvous.

M is the mass of the SSc.

is the mass of the sub-spacecraft.

For SSc, after release the sub-spacecraft, the velocity of SSc will change. We can get the expression of SSc' velocity is:

$$\mathbf{v}^M = \Delta\mathbf{v}_i\frac{m}{M+m} + \mathbf{v}^M \tag{15}$$

Because of the support that the time to release sub-spacecraft can be ignored, so the position of SSc spacecraft will not change.

2.4 Rendezvous precise estimate

In this section, the transfer process of release error and observation error is investigated, the expression of the rendezvous error is given. Only the two most critical constraints in this problem are considered. The first is that the relative displacement of the sub-spacecraft at the end moment is 0, which guarantees the rendezvous. The second is that the magnitude of the released velocity is constant and only the direction of the velocity can be changed. Assuming all distribution of error is normal distribution.

Assume that the expression of $\Delta\mathbf{v}(\alpha,\beta)$:

$$\Delta\mathbf{v} = \Delta v\begin{bmatrix}\cos\alpha\cos\beta \\ \cos\alpha\sin\beta \\ \sin\alpha\end{bmatrix} \tag{16}$$

According to the general law of error propagation, the distribution of $(\alpha,\beta,\Delta v)$ is assumed to be normal with a covariance matrix of R, then the distribution of $\mathbf{r}_t$ is:

$$\Omega = \left(\frac{M}{M+m}\right)^2 B_{12} \begin{bmatrix} \frac{\partial \Delta \mathbf{v}^T}{\partial \alpha} \\ \frac{\partial \Delta \mathbf{v}^T}{\partial \beta} \\ \frac{\partial \Delta \mathbf{v}^T}{\partial \Delta v} \end{bmatrix}^T R \begin{bmatrix} \frac{\partial \Delta \mathbf{v}^T}{\partial \alpha} \\ \frac{\partial \Delta \mathbf{v}^T}{\partial \beta} \\ \frac{\partial \Delta \mathbf{v}^T}{\partial \Delta v} \end{bmatrix} B_{12}^T \tag{17}$$

Assuming that the covariance matrix of the observation error of $\mathbf{r}_0$ is Q, and the covariance matrix of the observation error of $\mathbf{v}'$ is G, then the covariance matrix of the total rendezvous error is :

$$\Omega = B_{11} Q B_{11}^T + B_{12} G B_{12}^T + \left(\frac{M}{M+m}\right)^2 B_{12} \begin{bmatrix} \frac{\partial \Delta \mathbf{v}^T}{\partial \alpha} \\ \frac{\partial \Delta \mathbf{v}^T}{\partial \beta} \\ \frac{\partial \Delta \mathbf{v}^T}{\partial \Delta v} \end{bmatrix}^T R \begin{bmatrix} \frac{\partial \Delta \mathbf{v}^T}{\partial \alpha} \\ \frac{\partial \Delta \mathbf{v}^T}{\partial \beta} \\ \frac{\partial \Delta \mathbf{v}^T}{\partial \Delta v} \end{bmatrix} B_{12}^T \tag{18}$$

For analytical observation, a coordinate system that its YZ plane perpendicular to the velocity of the sub-spacecraft at the time of rendezvous is set and make the center of mass of the target spacecraft as the origin of this frame. Transferring the rendezvous error distribution onto this frame. We can utilize $|\lambda_2 + \lambda_3|/2$ to expressing the quantity of rendezvous error, λ_2 and λ_3 is the matrix composed of the 2nd and 3rd rows and columns.

3. Planning model

3.1 NSGA-II algorithm

Multi-objective optimization is a challenging problem that involves finding the best trade-off solutions among conflicting objectives. Genetic algorithms are a popular class of metaheuristic algorithms that can efficiently explore the search space and find a set of Pareto-optimal solutions. However, genetic algorithms face some difficulties in maintaining the diversity and convergence of the population, especially when the number of objectives is large. To overcome these difficulties, several multi-objective genetic algorithms have been proposed in the literature, such as NSGA, SPEA, MOGA, and PAES.

One of the most widely used and successful multi-objective genetic algorithms is NSGA-II[11], which stands for Non-dominated Sorting Genetic Algorithm II. NSGA-II is an improved version of NSGA, which was proposed by Srinivas and Deb in 1994. NSGA-II was developed by Deb et al. in 2002 and has the following features:

For minimization problems, at the beginning, a parent population P_0 is created randomly. Then sort the individuals in P_0 by non-domination and calculate their fitness values. Next, binary tournament selection, recombination, and mutation operators are used to create an offspring population Q_0.

Algorithm 1 NSGA-II

$R_t = P_t \cup Q_t$.
$(F_1, F_2, \ldots, F_l)$ = fast-non-domination(R_t)
$P_{t+1} = \varnothing$ and $i = 0$
Until $|P_{t+1}| + |F_i| \leq N$
\\sort R_t into different fronts $F_1, F_2, \ldots, F_l$.
crowding distance for each individual in F_i.
$P_{t+1} = P_{t+1} \cup F_i$
$i = i + 1$
$Sort(F_i, \prec_n)$
$P_{t+1} = P_{t+1} \cup F_i[1 : N - |P_{t+1}|]$
Q_{t+1} = make-new-pop(P_{t+1})
\\Use binary tournament selection, recombination,
\\ and mutation operators to create an offspring
\\population Q_{t+1} from P_{t+1}.

The define of $\prec_n$ as follow: for individual i and individual j, if $i_{rank} \leq j_{rank}$ and $i_{distance} = j_{distance}$, we notate it as $i \prec_n j$. i_{rank} is the non-domination rank of individual i, $i_{distance}$ is the crowding distance of individual i.

More details of NSGA-II in reference[11].

3.2 Decision variables and constraints

To ensure that all constraints are satisfied, which is essential for the feasibility and quality of the solutions, we apply a simple correction method after applying the genetic operators (selection, crossover, and mutation) on each chromosome. If a decision variable violates the upper or lower bound (if any), it is set to the bound value. This method is easy to implement and effective for handling various types of constraints. All constraints are shown in (19).

$$\begin{cases} \sum_{i=1}^{n} t_i^f \leq T_{\max} \\ \sum_{i=1}^{n} |\Delta \mathbf{v}_i| \leq \Delta v_{\max} \\ \Delta t_i^f \geq \Delta t_{\min} \\ |\mathbf{r}_i^i| \geq d_{\min} \end{cases} \tag{19}$$

3.3 Fitness function

The design of the fitness function is the key to the optimization problem. For the problem studied in this paper, the design of the fitness function is complex, and each calculation of the fitness function is equivalent to a complete dynamic simulation of the entire task process. The complete fitness function calculation process is shown in Figure 2. Where $\mathbf{r}_i^i$, $\mathbf{r}_i^{i+1}$ is the relative position of the SSc relative to the (i+1)th target spacecraft at the ith moment.

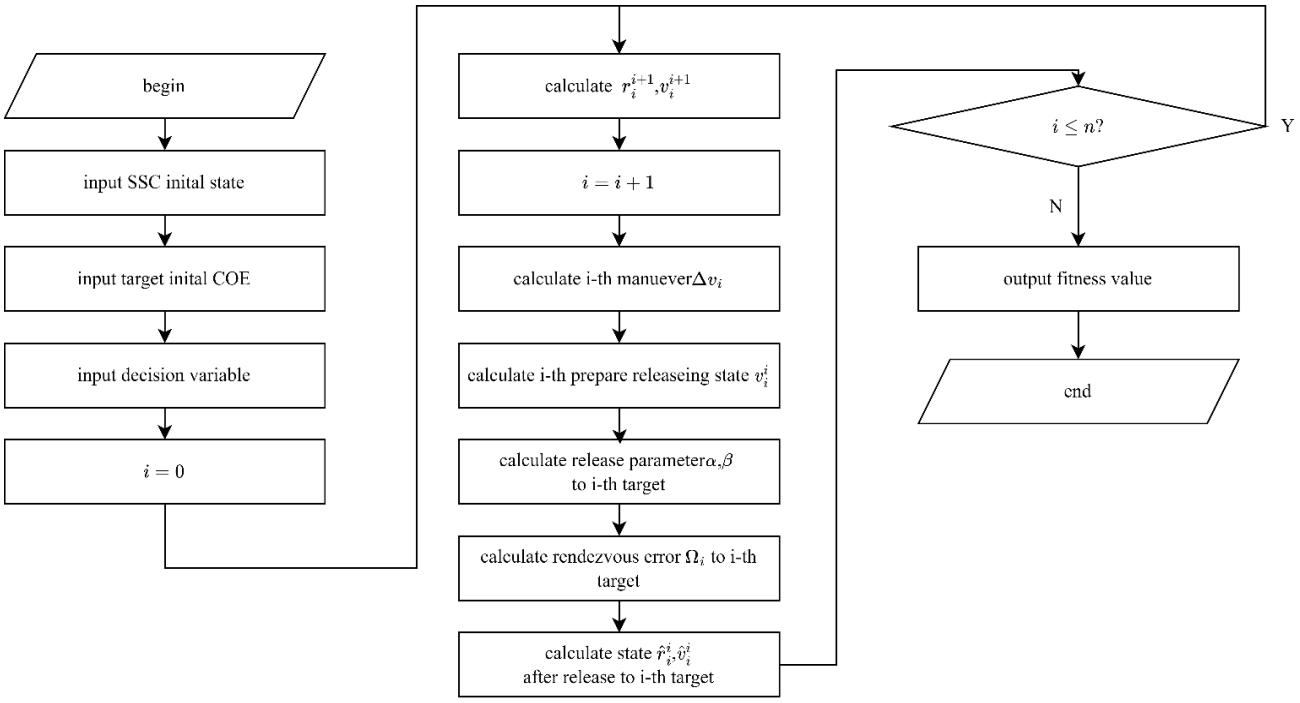

Figure 2. The processing of evaluate

4. Simulation example and discussion

In this paper, to verify the accuracy of the future verification planning model for elliptical orbit targets, we choose targets on the Molniya orbit as cases. A Molniya orbit is a class of highly elliptical orbits (HEO) that enable communication and remote sensing satellites to provide coverage over high-latitude regions. These orbits have an inclination of 63.4 degrees, an argument of perigee of 270 degrees, and an orbital period of approximately half a sidereal day. Satellites in the Molniya orbit have a long dwell time over the hemisphere they serve, while moving rapidly over the opposite hemisphere. This feature allows them to achieve a high elevation angle and a large footprint over high-latitude areas, where geostationary orbits (GEO) have poor performance and low Earth orbits (LEO) require a large constellation size. The Molniya orbit was first proposed and used by the Soviet Union in the 1960s for various civilian and military applications, such as television broadcasting, long-range communication, relay, weather monitoring, early warning systems and some classified purposes.

The initial orbital parameters of the target are given in Table 1.

Table 1. Initial orbit elements of targets spacecraft

object	a /km	e	i /deg	Ω /deg	ω /deg	f /deg
Target1	26600	0.74	63.4	0	270	0
Target2	26600	0.74	63.4	0	270	0.01
Target3	26600	0.74	63.4	0	270	0.02
Target4	26600	0.74	63.4	0	270	0.03
Target5	26600	0.74	63.4	0	270	0.04
Target6	26600	0.74	63.4	0	270	0.05
Target7	26600	0.74	63.4	0	270	0.06

4.1 Accompanying flight

In this case, we consider a co-orbiting configuration, where the SSc and the target satellites are

initially on close orbits with nearly equal velocities, and the SSc can maintain a quasi-stationary relative position to the target for an extended period of time. This configuration is useful for various purposes, such as inspection, rendezvous, docking, formation flying, or debris removal. We use NSGA-II, a multi-objective optimization genetic algorithm, to optimize the co-orbiting trajectory and control parameters under multiple constraints and objectives.

The initial state of the SSc relative to taget1 is given in Table 2.

Table 2. Initial state of SSc relative to target1

r_x /	/	/	v_x /	v_y /	/ ms^{-1}
-10000	r_y 0	10000	ms^{-1} 0	ms^{-1} 0	v_z 0

The change process of the minimum values of each fitness value with the number of iterations is shown in Figure 4. It can be seen that as the number of iterations increases, all indicators are decreasing, but the rate of decrease is slowing down and tends to converge.

By observing the distribution of the three fitness values: observation time, fuel, and average accuracy, we can find that fuel optimal and accuracy optimal are two relatively close optimization objectives, while time optimal is more contradictory to the other two. The reason is that when the SSc is close to the target, releasing the sub-spacecraft, the sub-spacecraft’ s flight time is shorter, and the rendezvous error of the sub-spacecraft is positively correlated with the flight time. When making a larger maneuver to quickly approach the target, it is beneficial to improve the accuracy.

We select all individuals whose average rendezvous error of sub-spacecraft is less than 1m from the final results, a total of 20, and plot their positions of releasing sub-spacecraft in the VVLH coordinate system of the first target and connect them with lines, as shown in Figure 5. The color of the line represents the size of the average rendezvous error of the individual on this diagram. The darker and bluer the color, the higher the average rendezvous accuracy, and vice versa. In the diagram, the five-pointed star represents the initial position of SSc, while the triangle indicates the position of the target.

By observing the release position diagram, it can be found that SSc with higher rendezvous accuracy tend to fly in the negative direction of the y-axis and turn back at the next time, and there is a trend that the farther they fly along the y-axis, the higher their accuracy. By plotting the release position diagram of all individuals and comparing it with those whose average error is within 1m, it can be found that in contrast, for individuals with lower fuel consumption, they usually follow the target queue near the target and usually do not fly too far. Figure 4 also shows the relative release position diagrams of the individuals who are optimal for each indicator. By observing, we can find that for the individuals who are optimal for time and accuracy, their strategy patterns are similar, but very different from the individual who is optimal for fuel.

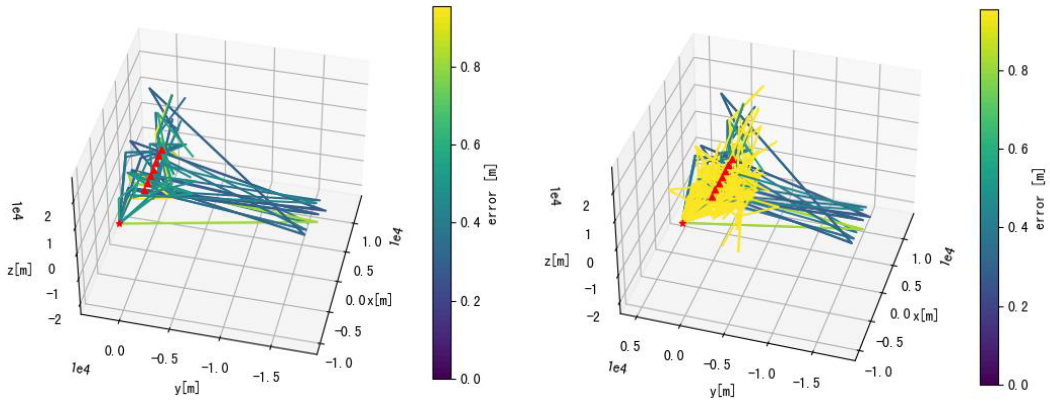

(a) The individual mean error less than 1m (b) All individuals

Figure 3. The position to release sub-spacecraft of SSc
(the color bar in the right present the mean error to all targets)

In practical engineering, we expect more comprehensive strategy schemes for multiple aspects of

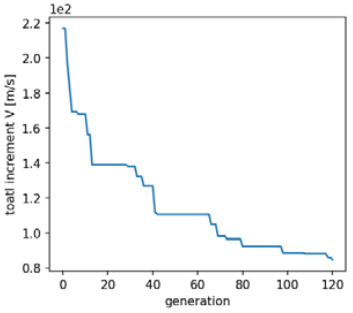

(a) Total consume of increment of velocity

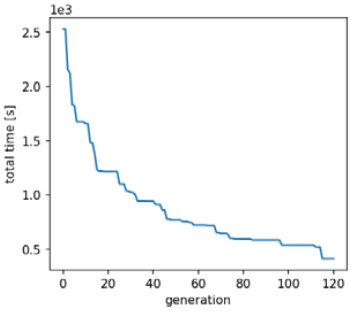

(b) Mean rendezvous error to all targets

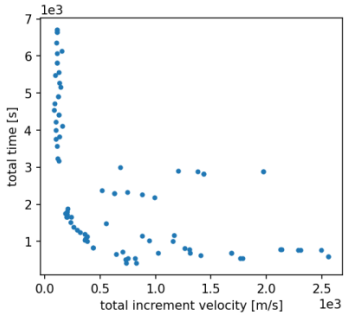

(c) Fitness of total time and total increment of velocity

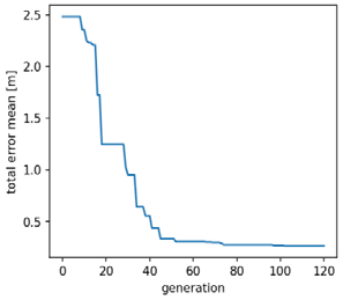

(d) Total consume of time

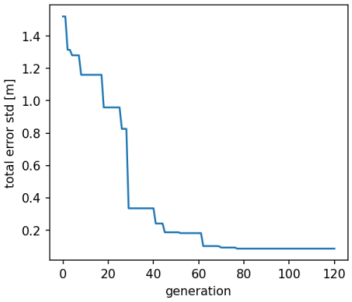

(e) Standard deviation of rendezvous error to all targets

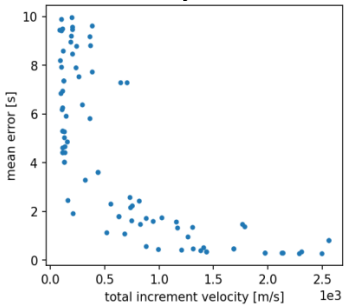

(f) Fitness of mean and total increment of velocity

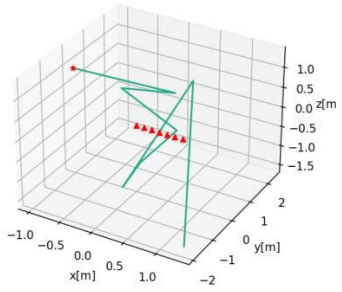

(g) Release position of fuel greatest strategy

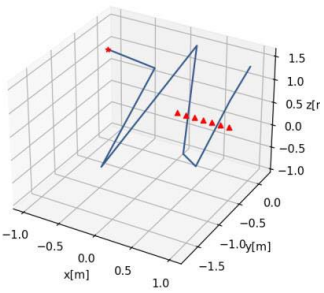

(h) Release position of error greatest strategy

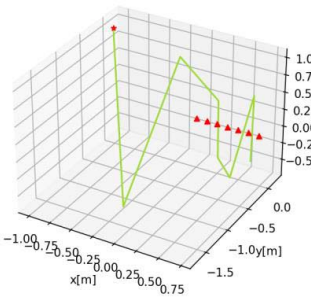

(i) Release position of time greatest strategy

Figure 4. The detail diagram for Accompanying flight

indicators. Therefore, we can set reasonable schemes and select suitable individuals from the Pareto frontier. This paper tries to give a more reasonable scheme. For the accuracy indicator, it only needs to be less than a certain upper limit, and we first screen out the individuals that meet the given accuracy and then further consider. For the time indicator and fuel indicator, we can use a linear weighted form to fuse them into one indicator. The specific weights of the two indicators can be selected according to the actual situation. For tasks with high timeliness requirements, the time indicator can be set larger, and other tasks take a larger weight of fuel consumption.

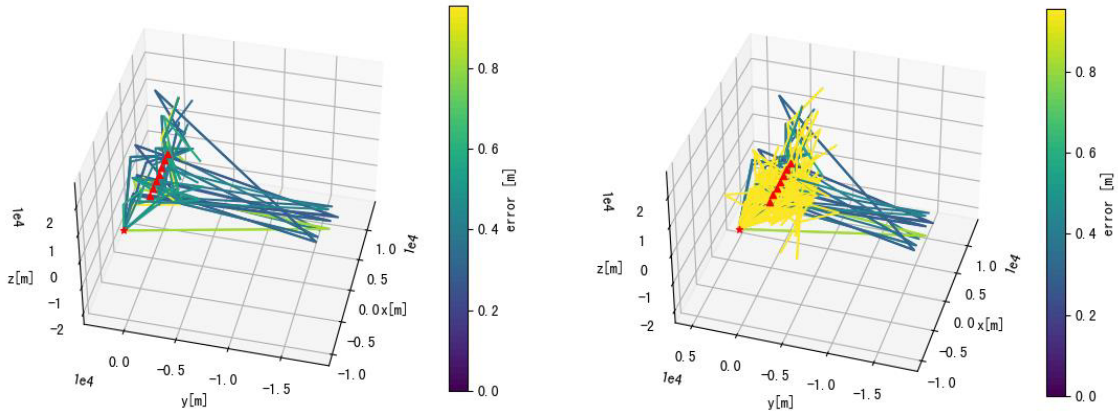

(a) The individual mean error less than 1m (b) All individuals

Figure 5. The position to release sub-spacecraft of SSc
(the color bar in the right present the mean error to all targets)

Table 3. The rendezvous error of each target

object	Mean error
Target1	1.24947138
Target2	1.78068709
Target3	1.87266277
Target4	1.91786643
Target5	2.66718079
Target6	4.66488995
Target7	3.37200286

We calculate the average rendezvous error of all individuals for each target, and the results are shown in Table 3. It is easy to find that the later the individual, the larger the rendezvous error, and vice versa. From the perspective of the target formation, the spacecraft closer to the SSc are easier to be cleaned more efficiently, while the spacecraft behind can use the cover of the front spacecraft to reduce the probability of being cleaned.

4.2 Glancing flight

In this case, we consider a glancing flight configuration, where the SSc and the target satellite are initially within a certain range of distance, but have significantly different velocities, and the SSs will rapidly fly past the target spacecraft. This configuration is useful for various purposes, such as reconnaissance, surveillance, imaging, or sampling. The initial orbital parameters of the target are given in Table 1. The initial state of the SSc relative to taget1 is given in Table 4. The optimizing process is shown in Figure 6.

Table 4. Initial state of SSc relative to target1

$r_x/$	$r_y/$	r_z/m	v_x/ms^{-1}	v_y/ms^{-1}	v_z/ms^{-1}
-10000m	0_m	10000	300	0	0

For the glancing flight scenario, we plot the relative release position diagrams of the individuals whose average rendezvous error of sub-spacecraft is less than 0.7m and less than 7m, respectively in Figure 7. The coordinate system is the VVLH coordinate system of target 1. In the diagram, the five-pointed star represents the initial position of SSc, while the triangle indicates the position of the target.

For the glancing flight scenario, the relative positions for high-accuracy rendezvous are more concentrated and regular. At the beginning, the SSc uses its large initial relative velocity to approach the target formation in the positive direction of the y-axis. In the later stage, the influence of the initial relative velocity becomes smaller, and the SSc also starts to enter a state of left and right glancing flight. The relative velocity along the formation direction is similar to that of the target formation.

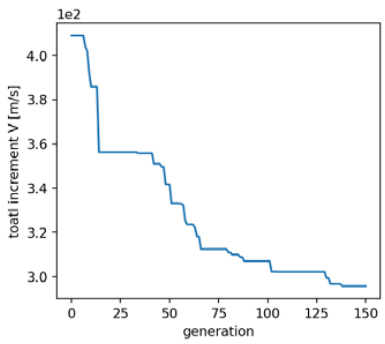

(a)Total consume of increment of velocity

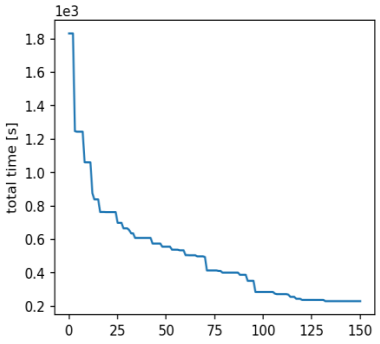

(b)Mean rendezvous error to all targets

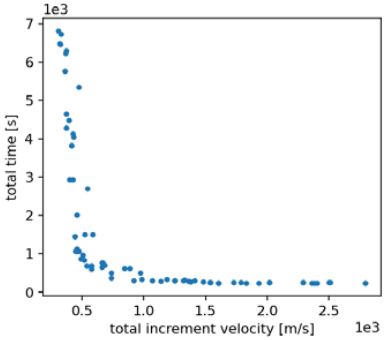

(c)Fitness of total time and total increment of velocity

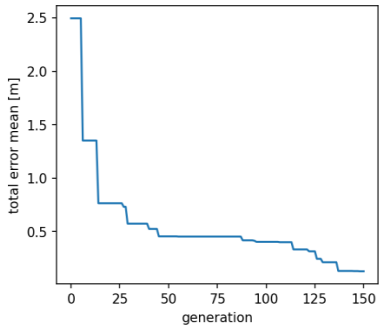

(d)Total consume of time

(e)

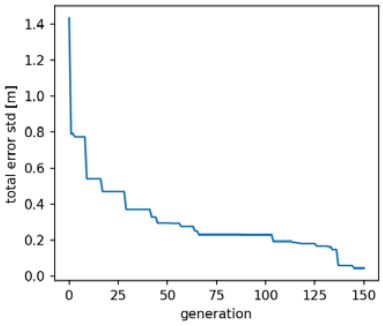

(f)Standard deviation of rendezvous error to all targets

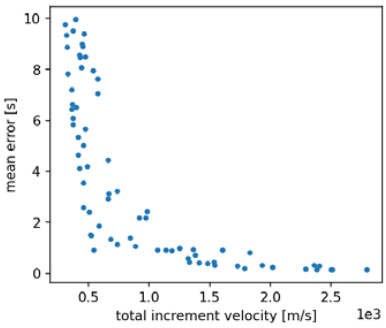

(g)Fitness of mean and total increment of velocity

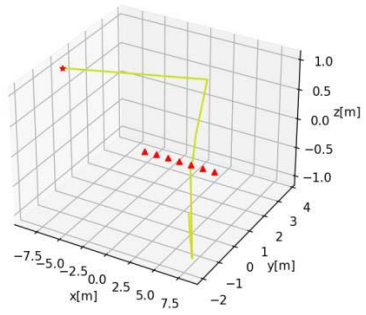

(h)Release position of fuel greatest strategy

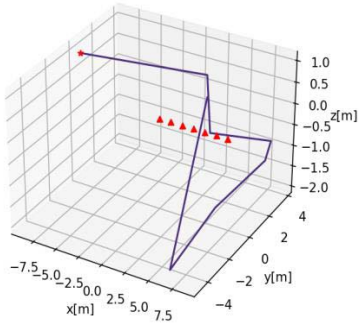

(i)Release position of error greatest strategy

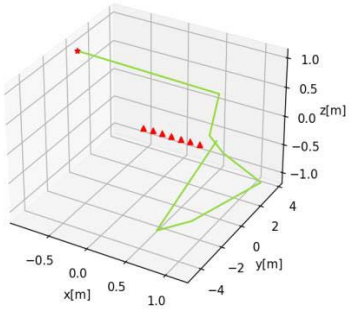

(j)Release position of time greatest strategy

Figure 6. the detail diagram for glancing flight

Table 5. The rendezvous error of each target

Object	Mean error
Target1	0.67102626
Target2	1.75170786
Target3	1.37338081
Target4	1.51002539
Target5	1.61526755
Target6	2.29115931
Target7	4.38365223

By comparing the accompanying scenario and the glancing flight scenario, we can find that glancing flight is more favorable for mission time, with shorter total flight time, while accompanying can achieve higher rendezvous accuracy overall. By observing the individuals who satisfy the average rendezvous error of less than 1m in the glancing flight scenario, we can also find that the individuals

who are optimal for time and accuracy have similar release positions, while they are quite different from the individual who is optimal for fuel consumption. However, the overall difference is smaller than that in the accompanying scenario. For the rendezvous effect, we can find that in the glancing flight scenario, the error of different targets being rendezvoused is also highly related to their initial distance from the SSc, in Table 5. Moreover, the correlation is greater than that in the accompanying scenario, especially for the last one with a larger error.

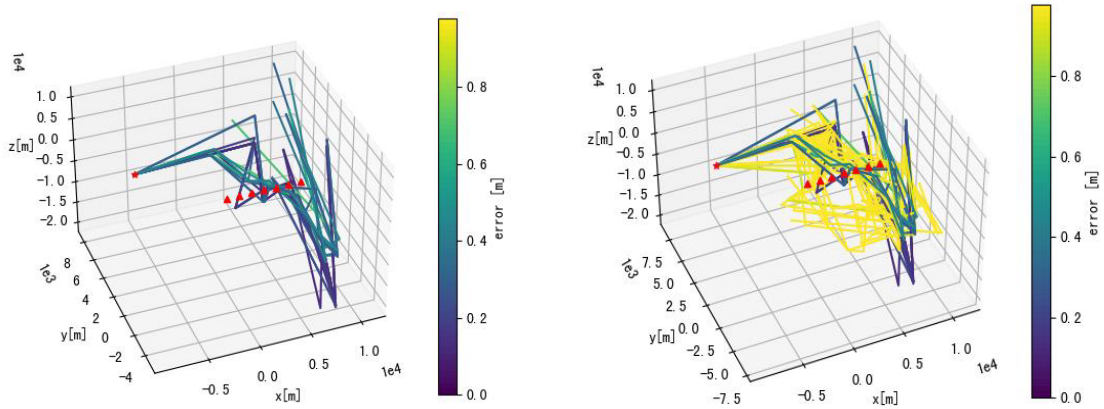

(a) The individual mean error less than 0.7m (b) The individual mean error less than 7m

Figure 7. The position to release sub-spacecraft of SSc
(the color bar in the right present the mean error to all targets)

5. Conclusion

This paper mainly studies the mission planning for the uncontrolled rendezvous of sub-spacecraft released, and conducts a series of research. First, the uncontrolled rendezvous process for elliptical orbit targets is analyzed and dynamically modeled. The contents such as maneuver, sub-spacecraft release parameter solution, rendezvous accuracy estimation are studied. Then, the NSGA-II algorithm is used to establish the mission planning model, focusing on the design of decision variables, constraints and fitness functions. Finally, through two specific cases of Molniya orbit, the effectiveness of the planning model is verified, and the planning results are deeply analyzed. The commonalities of a series of excellent strategies are summarized, which provide reference for the mission planning design of related tasks.

Through the analysis of the cases results, we find some characteristics of the uncontrolled rendezvous mission: first, time and accuracy are relatively close indicators, while fuel consumption is more contradictory to them. The individuals who are optimal for time and accuracy have higher fuel consumption and lower time consumption, while the individuals who are optimal for fuel consumption are just the opposite. Second, the SSc should actively create a “glancing flight” scenario. In the analysis of accompanying flight and glancing flight scenarios, the SSc has a tendency to flyby left and right. For the initial state of the scenario, the glancing flight initial scenario is better than the accompanying scenario, especially the total time consumption can reach a lower level. Finally, for the target formation, the spacecraft in the formation closer to SSc at the initial moment are more likely to be successfully cleaned. The error and order of rendezvous are approximately positively correlated. Moreover, the correlation of glancing flight scenario is greater than that of accompanying scenario.

References

[1] YAMANAKA K, ANKERSEN F. New state transition matrix for relative motion on an arbitrary elliptical orbit[J]. Journal of Guidance, Control, and Dynamics, 2002, 25(1): 60-66.

[2] MA Y H. CW guidance error analysis[J]. Aerospace Control, 2009(5): 38-42.

[3] JEYAKUMAR D, NAGESWARA RAO B. Dynamics of satellite separation system[J]. Journal of Sound and Vibration, 2006, 297(1-2): 444-455.

[4] CUI D, ZHANG Y, WANG J, et al. Analysis of parameter sensitivity on dynamics of satellite separation[J]. Acta Astronautica, 2015, 114: 22-33

[5] European Space Agency. ESA's Space Environment Report 2022[EB/OL]. https://www.esa.int/Space_Safety/Space_Debris/ESA_s_Space_Environment_Report_2022 .

[6] WANG J, ZHANG Y. Research on space target on-orbit capturing methods[C]//Journal of Physics: Conference Series. 2019, 1168(3): 032020.

[7] AN H, GUO Y, LI C, et al. Neural-network-assisted optimization of a close-range multi-spacecraft rendezvous mission based on a multi-impulse maneuvering strategy[J]. Advances in Space Research, 2023, 72(1): 1-15.

[8] FAN G, BAI L, WEI C, et al. Analysis and simulation of spacecraft on-orbit release safety[J]. Spacecraft Environment Engineering, 2017, 34(4): 403-409.

[9] LI H, PENG Q, ZHOU Y, et al. Orbit determination accuracy research for Chang'e-5 probe rendezvous and docking segment[J]. Scientia Sinica Physica Mechanica & Astronomica, 2021, 51(11): 66-77.

[10] XIE L, TANG G, ZHANG Y, et al. TG01/SZ08 rendezvous and docking orbit determination and prediction accuracy analysis[J]. Journal of Telemetry Tracking and Command ,2013(2):6.

[11] DEB K, PRATAP A, AGARWAL S, et al. A fast and elitist multiobjective genetic algorithm: NSGA-II[J]. IEEE Transactions on Evolutionary Computation ,2002 ,6 (2) :182-197.

[12] CHEN X Q, YU J. Optimal mission planning of geo on-orbit refueling in mixed strategy[J]. Acta Astronautica ,2017 ,133 :63-72.